

Friction stir welding of recycled A6061 aluminum plates fabricated by hot-extrusion of machined chips

ICHINORI SHIGEMATSU*, KAZUTAKA SUZUKI, TSUNEMICHI IMAI, YONG-JAI KWON, NAOBUMI SAITO

Institute for Structural and Engineering Materials (ISEM), National Institute of Advanced Industrial Science and Technology (AIST), 2266-98, Anagahora, Shimoshidami, Moriyama-ku, Nagoya, Aichi 463-8560, Japan
 E-mail: i-shigematsu@aist.go.jp

An excellent process for saving energy and resources is the ‘solid phase recycling process’ [1–5], since it can process material at lower temperatures and with a higher recycled product yield than the more common remelting processes used currently. This technique consolidates machined chips in the solid phase by a hot-extrusion process. Lightweight metals made by the solid phase recycling process have a fine structure due to severe plastic deformation during the production process. Material shapes, however, are restricted to thin solid cylinders or narrow strips because of processing constraints. Therefore, in order to make large-size components it is necessary to use secondary processing such as joining.

Generally, melting-type welding methods are employed for joining lightweight metals. These methods, however, significantly impair the structure because of inevitable grain coarsening and segregation of alloying elements.

Friction Stir Welding (FSW) has emerged as a new solid state joining technique [6], especially for aluminum alloys [7–14]. In this process, a rotating tool travels down the length of contacting metal plates, and produces a highly plastic deformed zone through the associated stirring action. Friction between the tool shoulder and the plate top surface produces a localized heating zone, an addition to the plastic deformation of the material brought by contact with the tool.

In this research, solid phase recycled materials were friction stir welded in the solid state in order to obtain plate materials with superior mechanical properties. The structure of FSW specimens was analyzed using a scanning ion microscope (SIM, Seiko Instruments Inc. SMI-2000) and a transmission electron microscope (TEM, Hitachi, Ltd. H-800).

Fig. 1 shows machined chips of A6061. These were prepared by machining an extruded A6061 rod using a lathe with no lubricant. The machined chips were encapsulated in a pure aluminum can, and extruded with an extrusion ratio 1:4 at 873 K. As a result, cylindrical recycled materials with a diameter of about 20 mm were obtained. The materials were rolled perpendicular to the extrusion direction (in the diametral direction) at 673 K to give plate specimens 100 mm × 60 mm × 4 mm in size. Specimen surfaces that contacted the

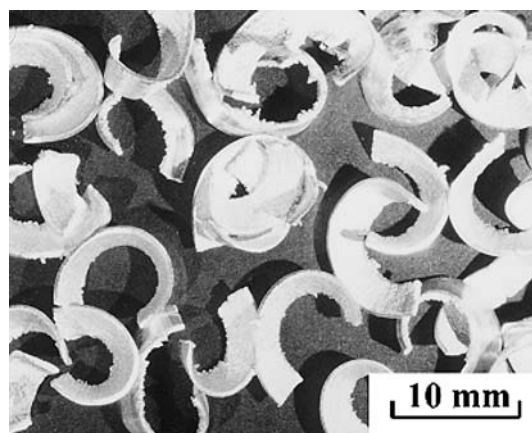


Figure 1 Machined chips of A6061 alloy.

FSW tool were left in the as-rolled condition. Two plate specimens were placed parallel to each other for joining. The tool for the FSW was made by SKD61. The tool's shoulder and insert pin diameters were 13 mm and 3 mm, respectively. Joining was carried out at 1320 rpm with a travel speed of 2.0 mm/s.

Fig. 2 shows a reflected light micrograph of the A6061 plate cross-section prepared by hot-extrusion

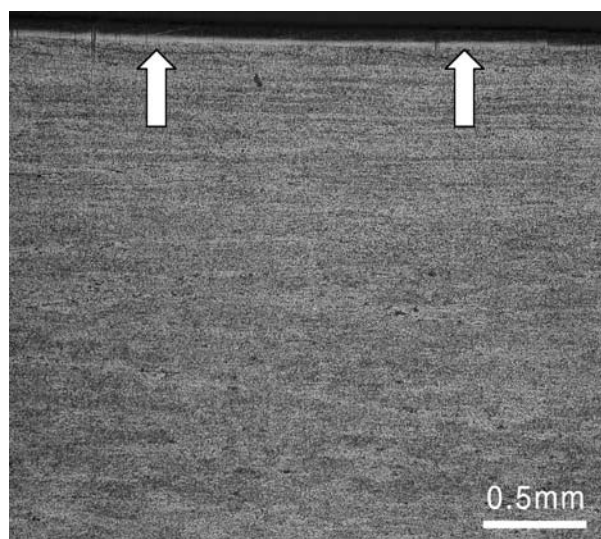


Figure 2 Reflected light micrograph of a cross-section of solid recycled A6061 aluminum alloy (Etched in Keller's reagent (HNO₃+HCl+HF)).

*Author to whom all correspondence should be addressed.

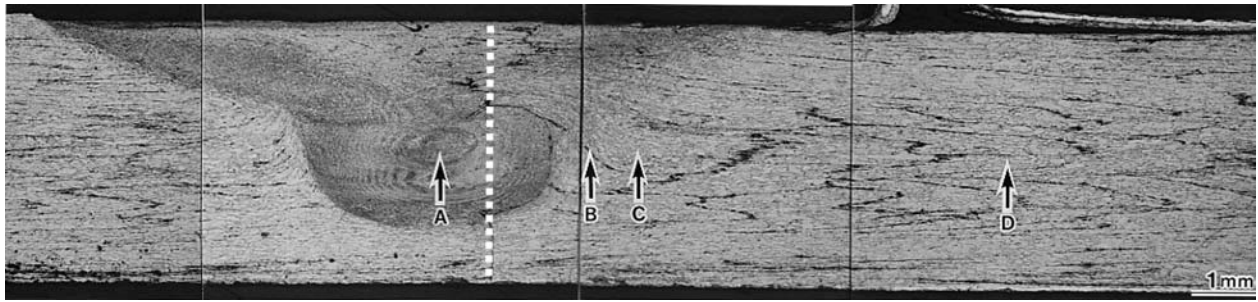


Figure 3 Cross-section of FSW specimen (Etched in Keller's reagent). (A) Center of friction stir zone, (B), (C) vicinity of the boundary between the friction stir zone and the base metal and (D) base metal. The white dot line indicates the boundary between two plates.

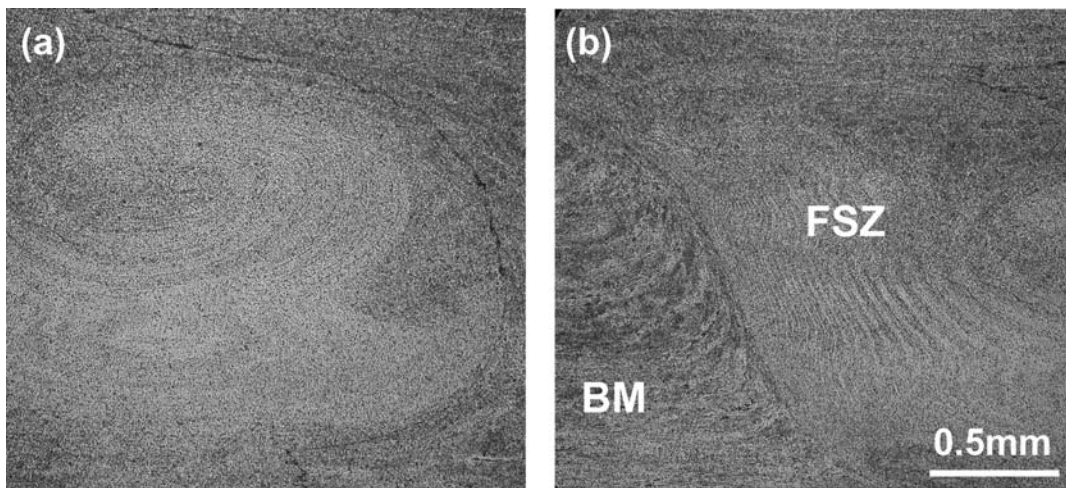


Figure 4 Reflected light micrographs of (a) center of friction stir zone and (b) boundary between the friction stir zone (FSZ) and base material (BM).

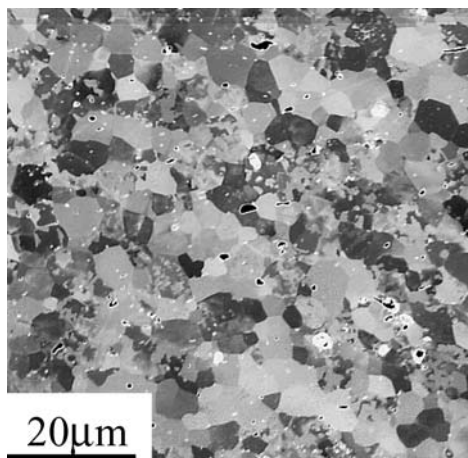


Figure 5 Photographs of scanning ion microscope at the center of friction stir zone. (Ga ion, 30 kV).

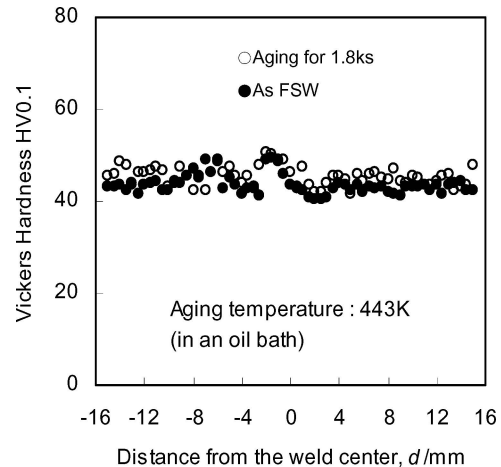


Figure 6 Hardness distributions of FSW A6061 specimen fabricated by solid phase recycling process.

of the machined chips followed by rolling. The pure aluminum that encapsulated the machined chips left an aluminum layer of about 0.1 mm thickness on the plate surface, which is indicated by white arrows in Fig. 2. The aluminum layers were left on the surfaces during joining. The insides of the specimens were well densified indicating that the machined chips were fully consolidated. Fig. 3 shows a cross section of FSW specimens. No defects were observed at the junction, which indicates that the joining quality was quite good. Fig. 4 shows detailed views of the center of friction stir zone (FSZ) and the vicinity of the boundary between the fric-

tion stirred zone and the base metal (BM). Although the base metal has a structure that is elongated in the rolling direction, the rolled structure was not observed in the friction stir zone due to severe plastic deformation by the FSW. Spiral metal flow was observed in the friction stir zone. Furthermore, many 'chip boundaries', which are oxide layers on chip surfaces, were observed in the base metal. In the friction stir zone, however, the chip boundaries disappeared because of breakage of oxide layers that compose the boundary. Although the structure showed a steep change in the vicinity of the boundary between the friction stir zone and the base metal,

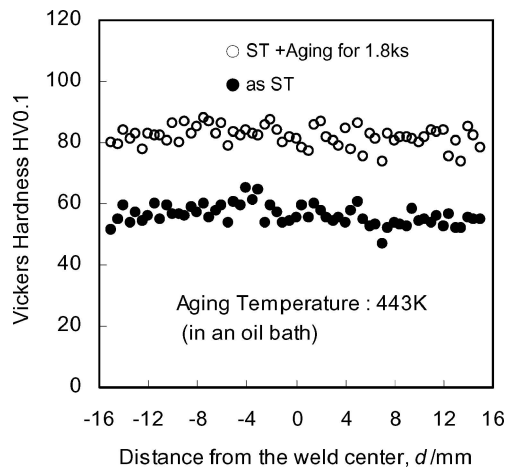


Figure 7 Hardness distributions of FSW specimen with a solution treatment (ST).

defects such as cracks were not present. Fig. 5 shows a scanning ion micrograph taken at the center of the friction stir zone. Equiaxed fine grains with diameters of 5–10 μm were observed. Fig. 6 shows the hardness distribution in the vicinity of the weld. The rolled base metal and the friction stir zone both had a hardness level of approximately HV45, showing no significant difference. No change in hardness was observed after a heat treatment at 443 K for 1.8 ks. Fig. 7 shows the changes in the hardness of the joined specimen after a solution treatment followed by a heat treatment at 443 K for 1.8 ks. No significant hardness difference was observed

between the friction stirred zone and the base metal. Therefore, it can be concluded that the structural difference between the friction stir zone and the base metal has little influence on aging behaviors. A hardness increase was not observed despite grain refinement; this was due to the dominant influence of precipitates rather than the grain size in the A6061 alloy. A TEM photograph of the FSW material is shown in Fig. 8. Both the friction stir zone and the base metal have a low dislocation density. Analysis of precipitates by energy dispersive X-ray spectroscopy (EDX) showed the presence of Fe-Al-base precipitates with a particle size not greater than 0.1 μm , and rod-shaped coarse Mg-Si-base precipitates with a size of 0.1–1 μm in both the friction stir zone and the base metal. These results indicate that the aging precipitates inside grains coarsened during the recycle material preparation process, and hence hardly contributed to an increase in hardness.

Solid phase recycled materials fabricated by hot extrusion of machined chips were welded in the solid state by FSW. Main results are as follows. (1) The friction stir zone of recycled A6061 plate consisted of equiaxed fine grains with diameter of 5–10 μm . (2) Many ‘chip boundaries’, which are oxide layers on chip surfaces, were observed in the base material. In the stir zone, however, the chip boundary was not observed, apparently because of breakage of oxide layers that compose the boundary. (3) No significant hardness difference was observed between the friction stirred zone and the base metal due to post-welding heat treatment.

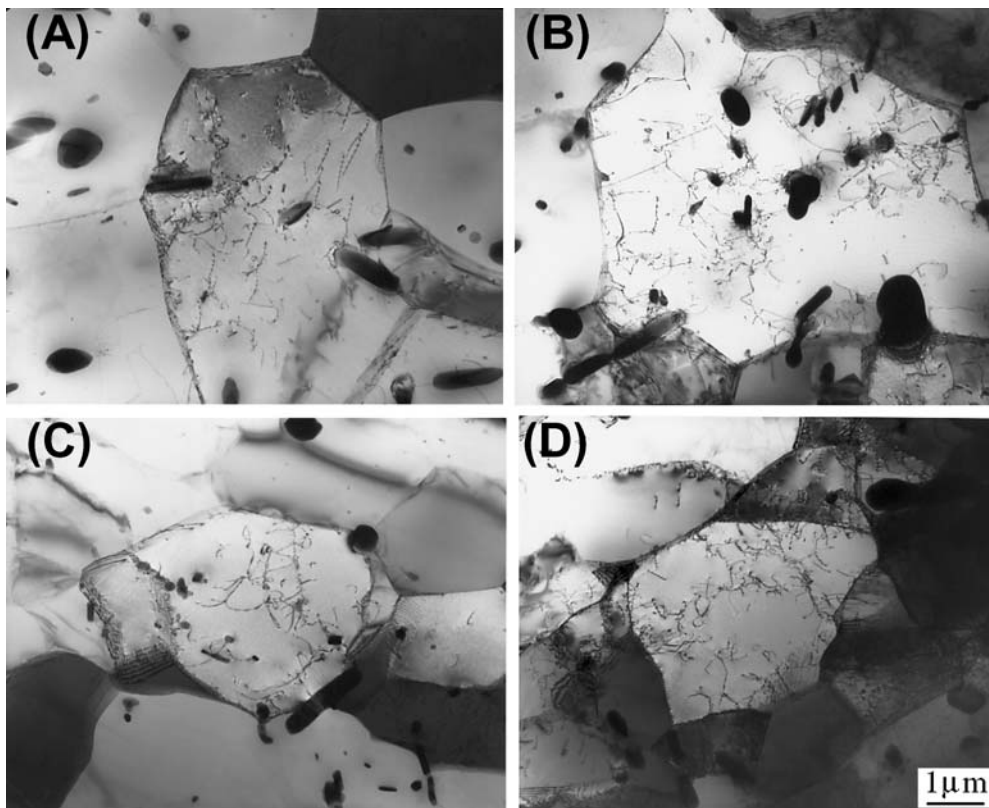


Figure 8 TEM images of FSW specimen. (A), (B), (C) and (D) show the detail images at point A, B, C and D in Fig. 1, respectively. (A) the center of friction stir zone, (B), (C) the vicinity of the boundary between the friction stir zone and the base metal and (D) base metal.

References

1. Y. CHINO, R. KISHIHARA, K. SHIMOJIMA, H. HOSOKAWA, Y. YAMADA, C. WEN, H. IWASAKI and M. MABUCHI, *J. Jpn. Inst. Metals* **65** (2001) 621.
2. *Idem.*, *Mater. Trans.* **43** (2002) 2437.
3. M. MABUCHI, K. KUBOTA and K. HIGASHI, *Mater. Trans. JIM* **36** (1995) 1249.
4. M. NAKANISHI, M. MABUCHI, N. SAITO, M. NAKAMURA and K. HIGASHI, *J. Mater. Sci. Lett.* **17** (1998) 2003.
5. K. SUZUKI, I. SHIGEMATSU, Y. XU, T. IMAI and N. SAITO, *J. Jpn. Inst. Light Metals* **53** (2003) 554.
6. W. M. THOMAS, E. D. NICHOLAS, J. C. NEEDHAM, M. G. MURCH, P. TEMPLESMITH and C. J. DAWES, GB Patent Application No. 9125978.8, Dec. 1991, US Patent No. 5460317 (Oct. 1995).
7. L. E. MURR, G. LIU and J. C. McCLURE, *J. Mater. Sci. Lett.* **16** (1997) 1801.
8. G. LIU, L. E. MURR, C.-S. NIOU, J. C. McCLURE and E. R. VEGA, *Scripta Mater.* **37** (1997) 355.
9. C. G. RHODES, M. W. MAHONEY, W. H. BONGEL, R. A. SPURLING and C. V. BAMPTON, *ibid.* **36** (1997) 69.
10. V. FLORES, C. KENNEDY, L. E. MURR, D. BROWN, S. PAPPU, B. M. NOWAK and J. C. McCLURE, *ibid.* **38** (1998) 703.
11. M. W. MAHONEY, C. G. RHODES, J. G. FLINTOFF, R. A. SPURLING and W. H. BINGEL, *Metall. Mater. Trans. A* **29A** (1998) 1955.
12. Y. LI, L. E. MURR and J. C. McCLURE, *Mater. Sci. Eng. A* **271** (1999) 213.
13. *Idem.*, *Scripta Mater.* **40** (1999) 1041.
14. I. SHIGEMATSU, Y. KWON, K. SUZUKI, T. IMAI and N. SAITO, *J. Mater. Sci. Lett.* **22** (2003) 353.

*Received 3 March
and accepted 14 October 2004*